

# Data charts and organization of data files

## 1 Organization of data files

### 1.1 Naming scheme

Data files with simulation results are named according to the following scheme (Pattyn et al., 2008):

NNNMELLL.txt

Placeholders have the following meaning:

- NNN: short for the initials of the researcher who preformed the experiments (here: tsa)
- M: the number of models (here: 1)
- E: the experiment (here: B or D), and
- LLL: three numbers denoting the length of the modeled domain (005, 010, 020, 040, 080, 160)

Data files show output for all grid points in the horizontal for the domain from 0 to the model width L (or between 0 and 1 for scaled coordinates). All variables are taken either at the surface  $y_s$  or at the basis of the ice at  $y_b$ . The abbreviations for the study presented here and the comparison models are named accordingly (see Table 1). Because experimental data have been compiled by different authors, the abbreviations for this study are 'tsa1' (2D experiments of 'B' and 'D') and 'jla1' (all other experiments).

### 1.2 Symbols and axes

Symbol	Variable	Typical unit
$\tau_{xy}(y_b), \tau_{zy}(y_b)$	basal shear stress perpendicular to y	Pa
$v_x), v_z)$	velocity at ice basis, x- and z-component	m/a
$v_x), v_y), v_z)$	velocity at ice surface, x-, y-, and z-component	m/a
$\hat{x}, \hat{y}, \hat{z}$	normalized coordinates parallel ( $\hat{x}, \hat{z}$ ) and vertical ( $\hat{y}$ ) to the tilted surface	m

**Table S1: Symbols used in the diagrams below. For simplicity the y-axis is always the vertical axis, regardless of 2D or 3D setup**

### 1.3 Data files for experiment A

For Experiment A the following output has been compiled in each file in that order: the normalized x position, the normalized y position, the horizontal velocity in x direction at the surface, the horizontal velocity in y direction at the surface, the vertical velocity at the surface, the basal shear stress in x direction, the basal shear stress in y direction and the difference between the isotropic and the hydrostatic stress at the basis of the ice.

$$\hat{x} \quad \hat{z} \quad v_x(y_s) \quad v_y(y_s) \quad v_z(y_s) \quad \tau_{xy}(y_b) \quad \tau_{zy}(y_b) \quad \Delta p$$

### 1.4 Data files for Experiment B

For Experiment B the following output has been compiled in each file in that order: the normalized x position, the horizontal velocity at the surface, the vertical velocity at the surface, the basal shear stress and the difference between the isotropic and the hydrostatic stress at the basis of the ice.

For 3D experiments, values are given for a profile at  $\hat{z}=0.25$ :

$\hat{x}$	$v_x(y_s)$	$v_y(y_s)$	$\tau_{xy}(y_b)$	$\Delta p$
-----------	------------	------------	------------------	------------

For 2D experiments:

$\hat{x}$	$v_x(y_s)$	$v_y(y_s)$	$\tau_{xy}(y_b)$	$\Delta p$
-----------	------------	------------	------------------	------------

## 1.5 Data files for Experiment C

For Experiment C the following output has been compiled in each file in that order: the normalized x position, the normalized y position, the horizontal velocity in x direction at the surface, the horizontal velocity in y direction at the surface, the vertical velocity at the surface, the horizontal velocity in x direction at the base, the horizontal velocity in y direction at the surface, the basal shear stress in x direction, the basal shear stress in y direction and the difference between the isotropic and the hydrostatic stress at the basis of the ice.

$$\hat{x} \quad \hat{z} \quad v_x(y_s) \quad v_y(y_s) \quad v_z(y_s) \quad v_x(y_b) \quad v_y(y_b) \quad \tau_{xy}(y_b) \quad \tau_{zy}(y_b) \quad \Delta p$$

## 1.6 Data files for Experiment D

For Experiment D the following output has been compiled in each file and in the given order: the normalized x position, the horizontal velocity at the surface, the vertical velocity at the surface, the horizontal velocity at the basis, the basal shear stress and the difference between the isotropic and the hydrostatic stress at the basis of the ice.

$\hat{x}$	$v_x(y_s)$	$v_y(y_s)$	$v_x(y_b)$	$\tau_{xy}(y_b)$	$\Delta p$
-----------	------------	------------	------------	------------------	------------

## 1.7 Data files for Experiment E

For Experiment B the following output has been compiled in each file and in the given order: The normalized x position, the horizontal velocity at the surface, the vertical velocity at the surface, the basal shear stress and the difference between the isotropic and the hydrostatic stress at the basis of the ice.

$\hat{x}$	$v_x(y_s)$	$v_y(y_s)$	$\tau_{xy}(y_b)$	$\Delta p$
-----------	------------	------------	------------------	------------

## 1.8 Data files for Experiment F

For Experiment A the following output has been compiled in each file: The normalized x position, the normalized z position, the y position at the surface, the velocity in x direction, the velocity in y direction and the vertical velocity.

$$\hat{x} \quad \hat{z} \quad y_s \quad v_x(y_s) \quad v_y(y_s) \quad v_z(y_s)$$

## 2 Explanations to the diagrams

### 2.1 Experiment A

This is a 3D ice-stream experiment of flow over a bumpy bedrock surface. The presented results have been calculated on an adapted grid (compare text) with a mesh resolution of  $128 \times 64 \times 8$ . Compare text for further explanations and parameters.

The surface velocity is given in  $m/a$ , shear stress is given in  $kPa$ . Data is plotted in Figures S1 and S2. Each model size is shown separately and compared to previous results from full-Stokes solutions compiled in Pattyn et al. (2008) (see Table S2).

### 2.2 Experiment B

This is a 3D and 2D ice-stream experiment of flow over a rippled bedrock surface. The presented results have been calculated on an adapted grid (compare text) with a mesh resolution of  $128 \times 64 \times 8$  (jla1) and  $256 \times 64 \times 32$  (tsa2) for 3D experiments. The resolution in 2D is  $256 \times 128$ . Compare main text for further explanations and parameters.

The horizontal surface velocity is given in  $m/a$ , shear stress is given in  $kPa$ . Data is plotted in Figures S3 to S6 for 3D and 2D settings. Each model size is shown separately and compared to previous results from full-Stokes solutions compiled in Pattyn et al. (2008) in case of the 3D experiments (see Table S2). Diagrams with results of the 3D experiments compare them to the results of the 2D setup.

### 2.3 Experiment C

This is a 3D experiment. The bedrock topography is flat, but the basal friction coefficient is prescribed by a sinusoidal function. The mesh resolution is  $128 \times 64 \times 8$ . For further explanations see main text.

Velocities are given in  $m/a$ , shear stress and pressure is given in  $kPa$ . Data is plotted in Figures S5 and S6. Each model size is shown separately and compared to previous results from full-Stokes solutions compiled in Pattyn et al. (2008) (see Table S2).

### 2.4 Experiment D

This is a 2D ice-stream experiment. The results presented here have been calculated on an rectangular grid with a mesh resolution of  $375 \times 75$ . Parameters and explanations are given in the main text.

The horizontal velocity at the surface and at the basis of the ice sheet is given in  $m/a$ , shear stress in x-direction is given in  $kPa$ . Data is plotted in Figures S7, S8 and S9. Each model size is shown separately and compared to previous results from full-Stokes solutions compiled in Pattyn et al. (2008) (see Table S2).

### 2.5 Experiment E

Exp. E is an experiment along the central flowline of a temperate glacier in the European Alps and thus essentially a 2D experiment. The model input consists of the longitudinal surface and bedrock profiles of Haut Glacier d'Arolla, Switzerland (Blatter et al., 1998 and Pattyn, 2002). In a first experiment the ice is frozen to the ground. A second variant considers a narrow zone of zero traction close to the center. The mesh geometry has been adapted to the bedrock topography, the resolution is  $50 \times 50$ . Compare main text for parameters and further explanations.

The horizontal velocity at the surface and at the basis of the ice sheet is given in  $m/a$ , shear stress is given in  $kPa$ . Data is plotted in Figures S11 and S12. Each model size is shown separately and compared to previous results from full-Stokes solutions compiled in Pattyn et al. (2008) (see Table S2).

### 2.6 Experiment F

Experiment F is a 3D ice-stream experiment over a central Gaussian bump. The free surface is allowed to relax until a steady state is reached. The mesh resolution is  $240 \times 48 \times 240$ , and the mesh geometry has been adapted to the bedrock topography. Experiments are run with a slip ratio  $c = 0$ , which means that ice is effectively frozen to the ground. This experiment uses Newtonian viscosity, in difference to previous experiments. Compare main text for parameters and further explanations.

Figures S12 and S13 compare the results to two full-Stokes solutions compiled in Pattyn et al. (2008) and an analytical solution, contributed by Frank Pattyn (2022, personal communication). Surface height is given in  $m$ , velocity in  $m/a$ .

### 2.7 Comparison models

The data plots below compare the results of this study with previous full-Stokes solutions compiled in the reference paper by Pattyn et al. (2008).

Model	Dimensions	Method	Reference
tsa1	2	MPM	this study, based on Mansour et al. (2020)
jla1	2,3	MPM	this study, based on Mansour et al. (2020)
aas2	3	FE	unpublished
cma1	3	FE	Martín et al. (2004)
jvj1	3	FE	Johnson and Staiger (2007)
mmr1	3	FE	unpublished
oga1	3	FE	(Gagliardini and Zwinger, 2008)
rhi1	3	Sp	Hindmarsh (2004)
rhi3	3	Sp	Hindmarsh (2004)
ssu1	2	FE	Sugiyama et al. (2003)

**Table 1:** *Model: abbreviation used in Pattyn et al., (2008) and in the diagrams. Dimensions: model dimensions. Method: numerical method: FE = finite elements, Sp = spectral method, MPM = material point method.*

### 3 Diagrams for Experiment A

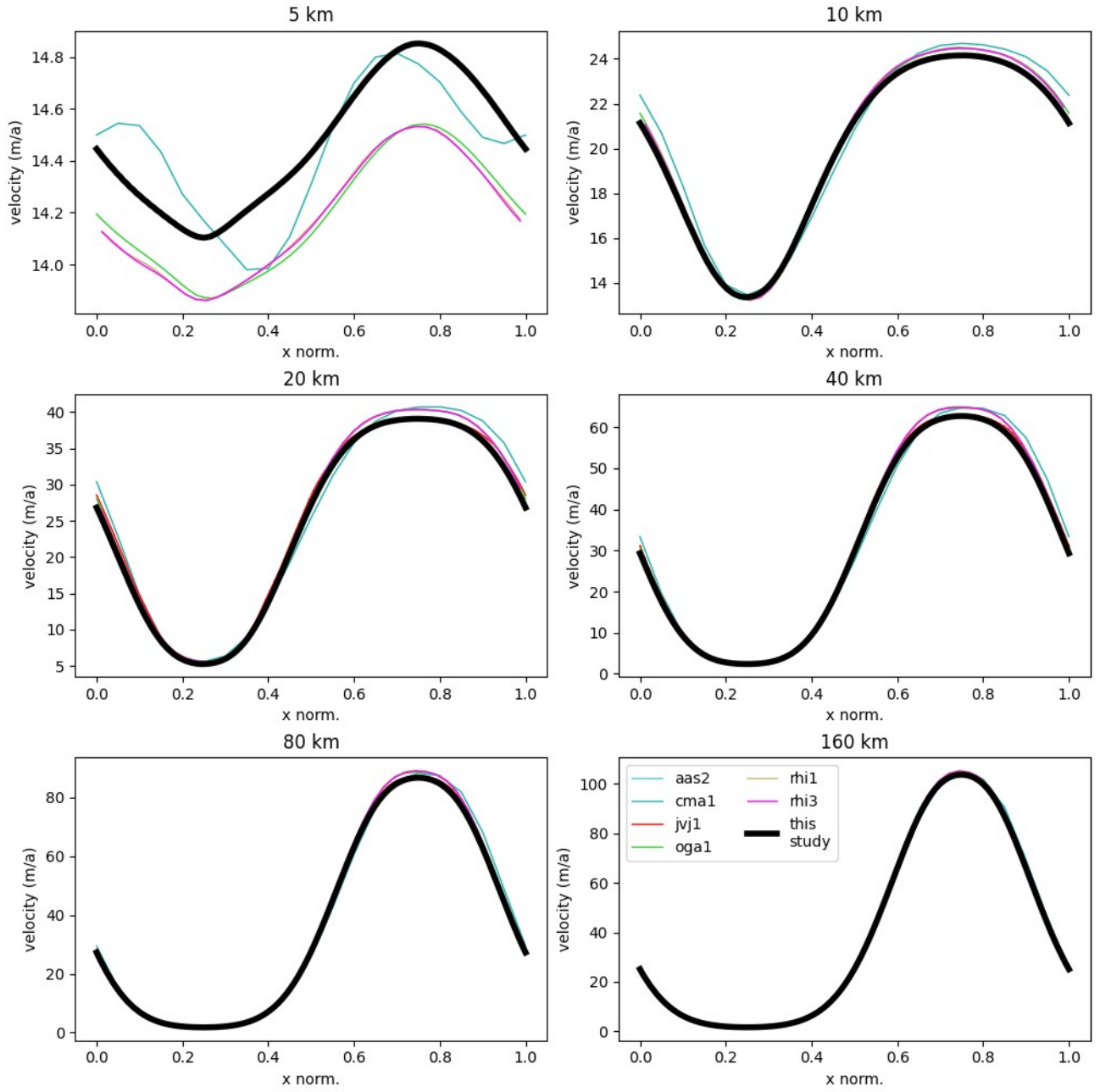
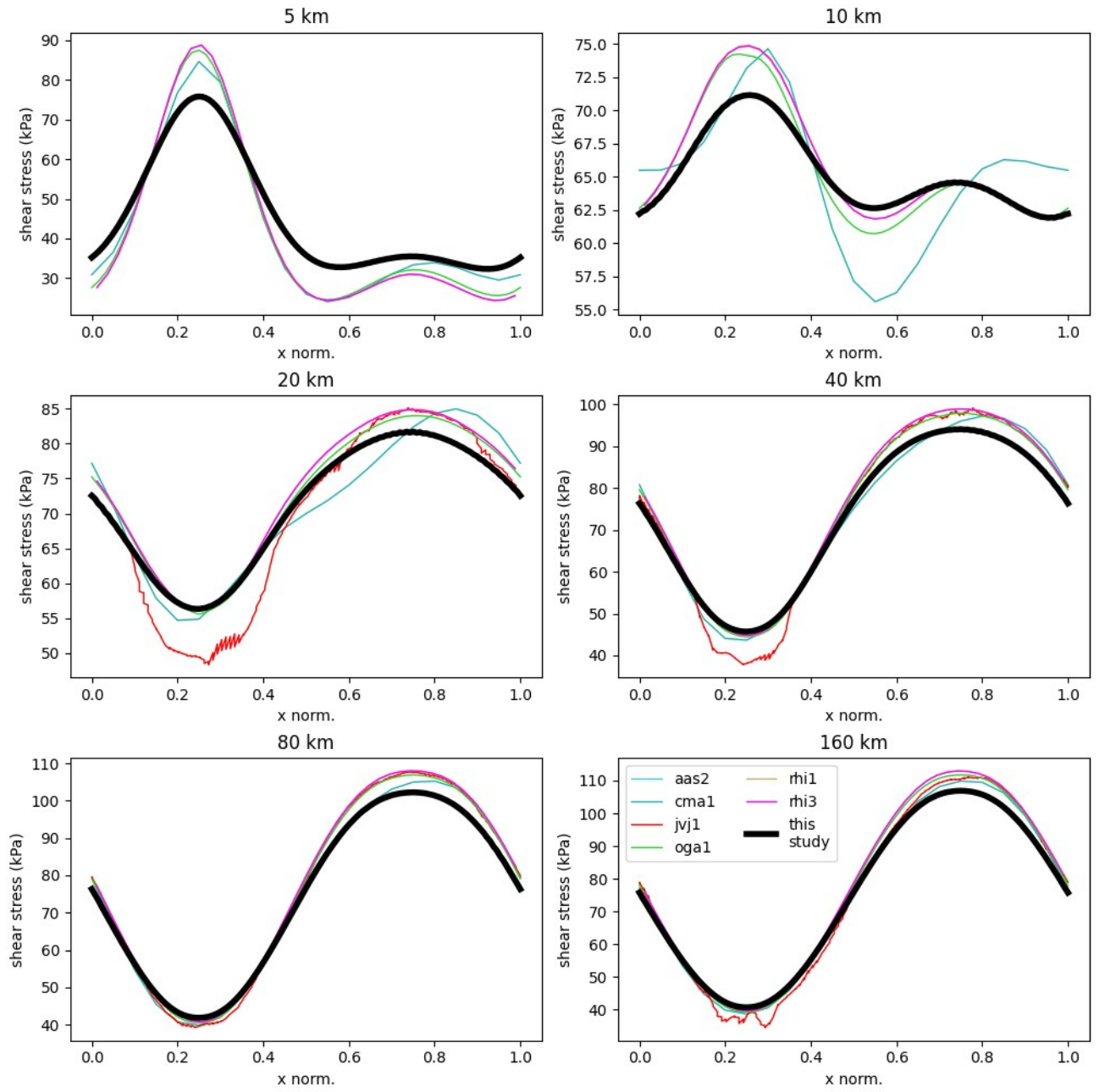


Figure S1: Experiment A. Surface velocity in x-direction  $V_x(y_s)$  at  $\hat{z} = 0.25$ . Black line: this study (jla1).



**Figure S2: Experiment A. Shear stress in x-direction at the basis,  $\tau_{xy}(y_b)$ . Black line: this study (jla1).**

## 4 Diagrams for Experiment B

### Experiment B - 2D results

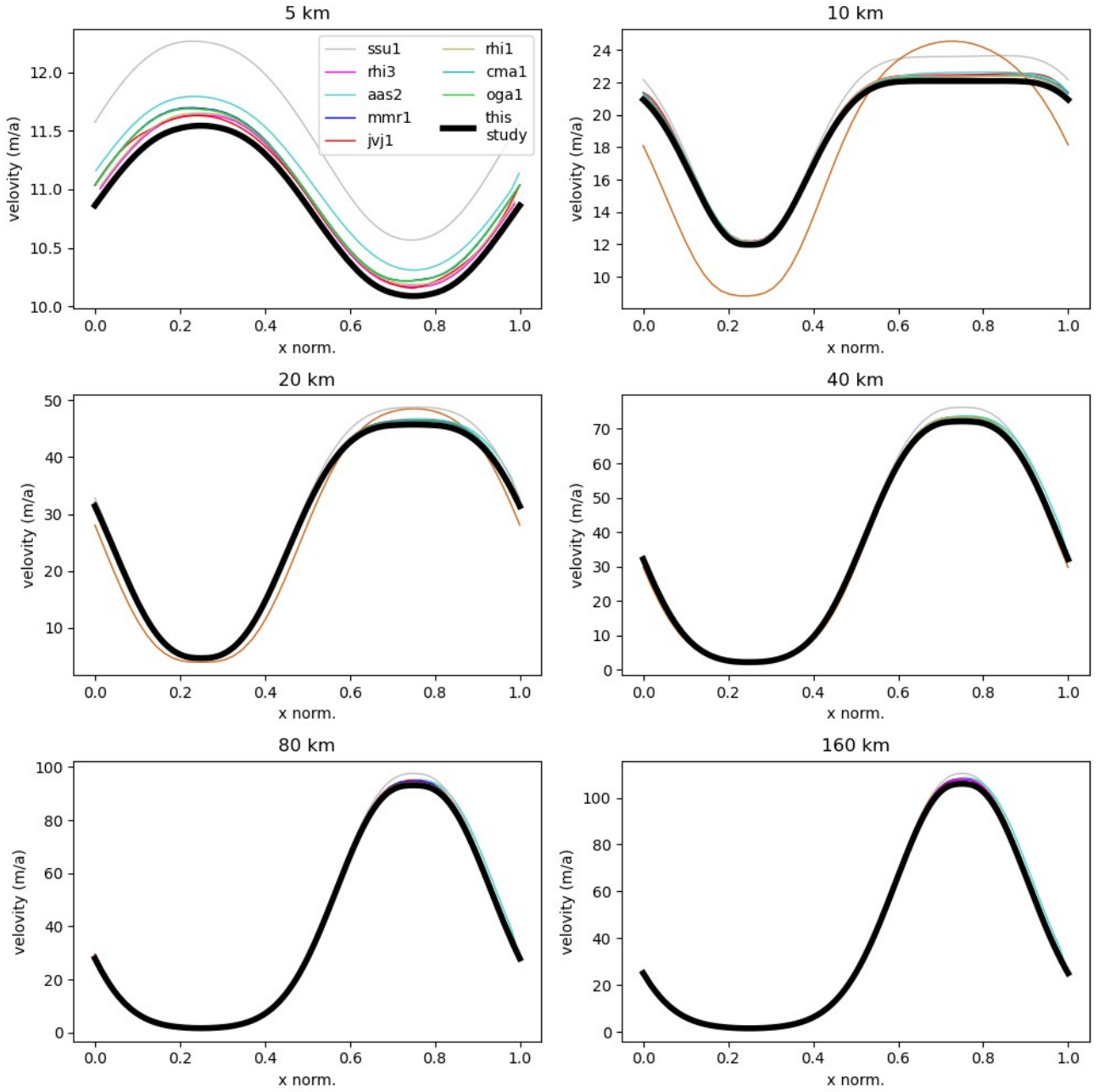
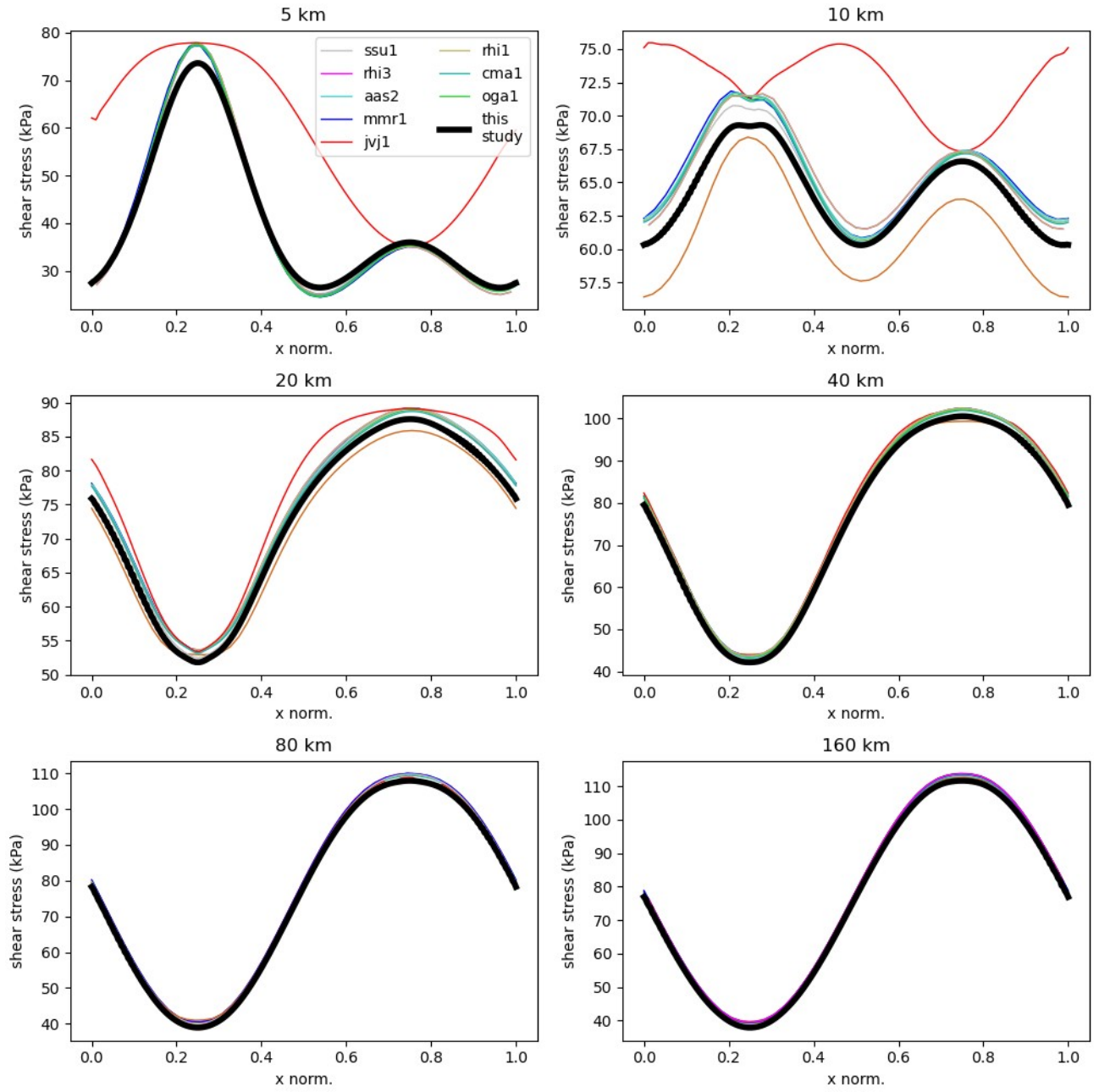


Figure S3: Experiment B (2D). Surface velocity in x-direction  $V_{xy}(\hat{y}_s)$  at  $\hat{z} = 0.25$ . Black line: this study (tsa1).



**Figure S4: Experiment B (2D),  $n=3$ . Shear stress in  $x$ -direction at the basis,  $\tau_{xy}(y_b)$ . Black line: this study (tsa1).**



## Experiment B - 3D results

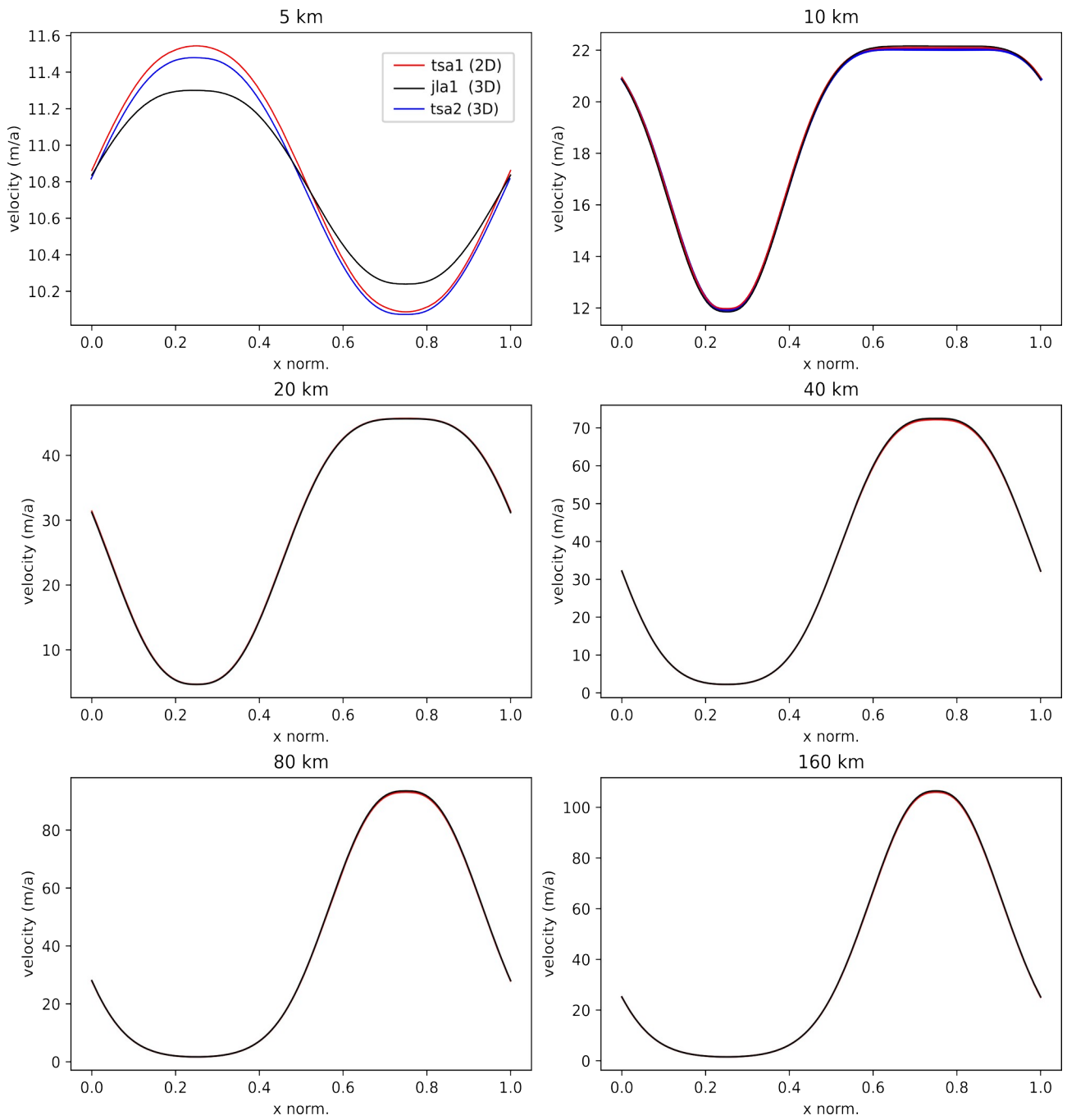


**Figure S5: Experiment B (3D).** Surface velocity in x-direction  $V_{xy}(y_s)$  at  $\hat{z} = 0.25$ . Black: 3D results (jla1) with  $128 \times 64 \times 8$ , blue: 3D results (tsa2) with  $258 \times 64 \times 32$ , red: 2D results (tsa1).

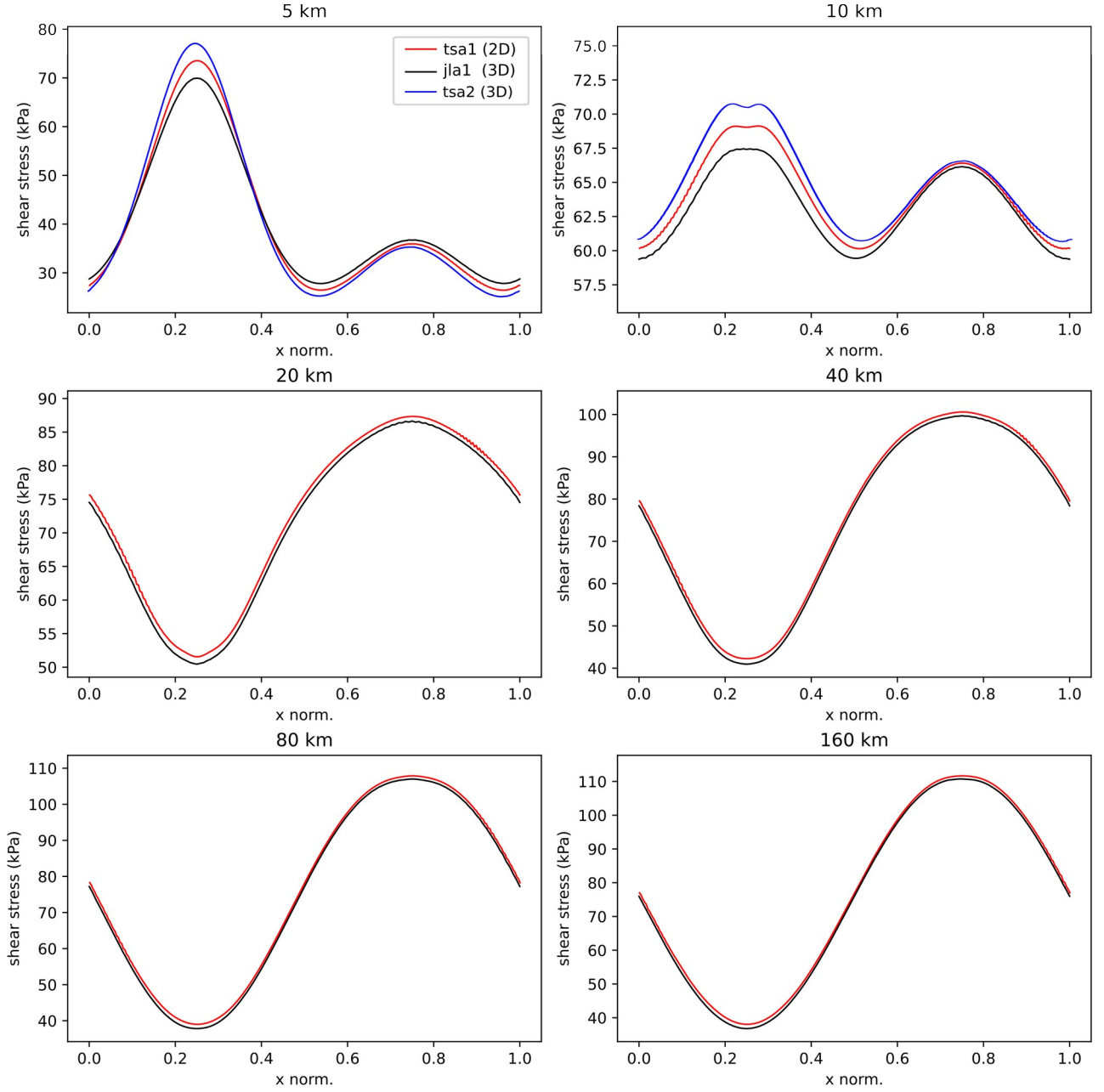


**Figure S6: Experiment B (3D). Shear stress in x-direction at the basis,  $\tau_{xy}(y_b)$  at  $\hat{z} = 0.25$ . Black: 3D results (jla1) with  $128 \times 64 \times 8$ , blue: 3D results (tsa2) with  $258 \times 64 \times 32$ , red: 2D results (tsa1).**

## 5 Diagrams for Experiment D

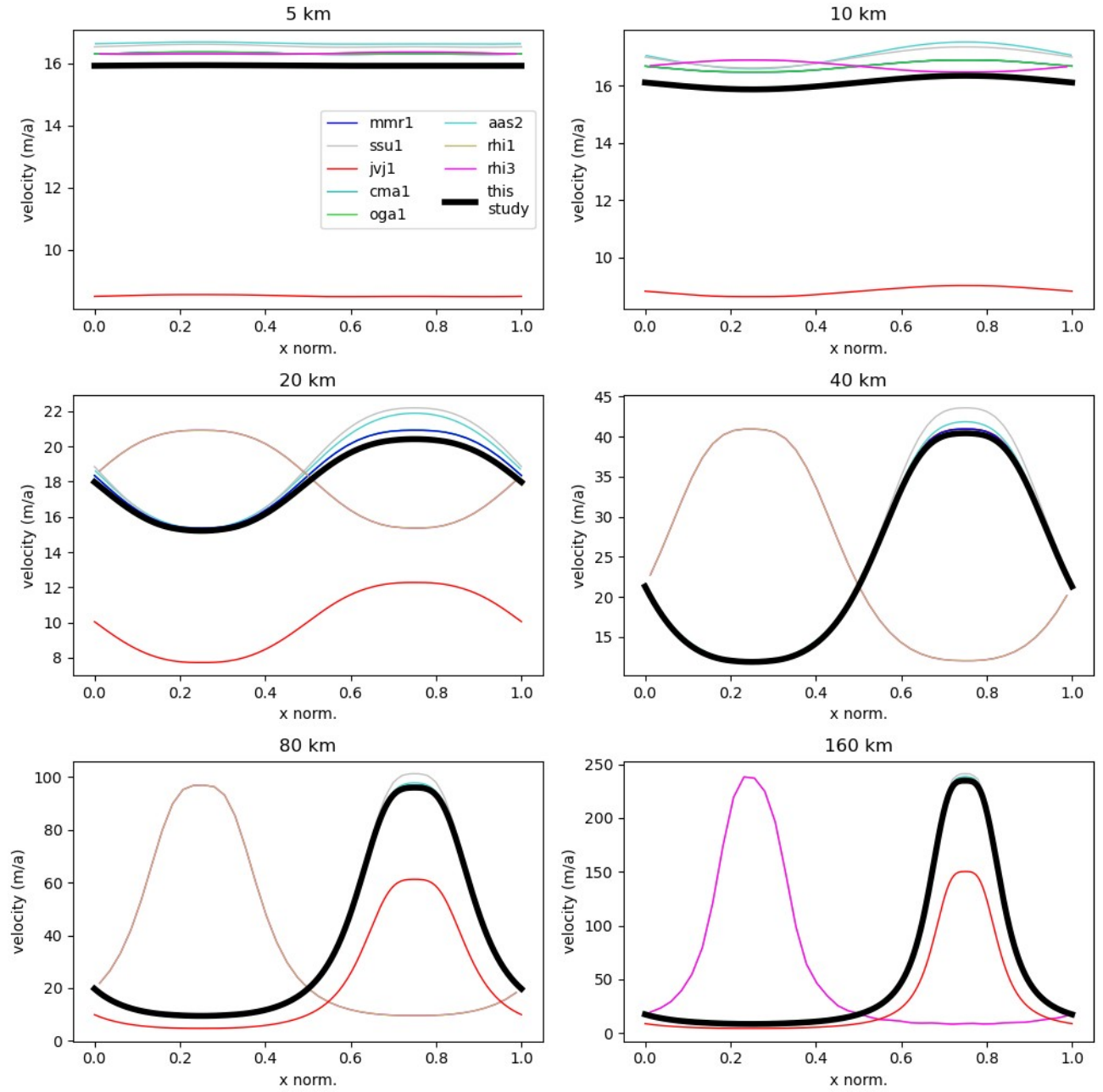
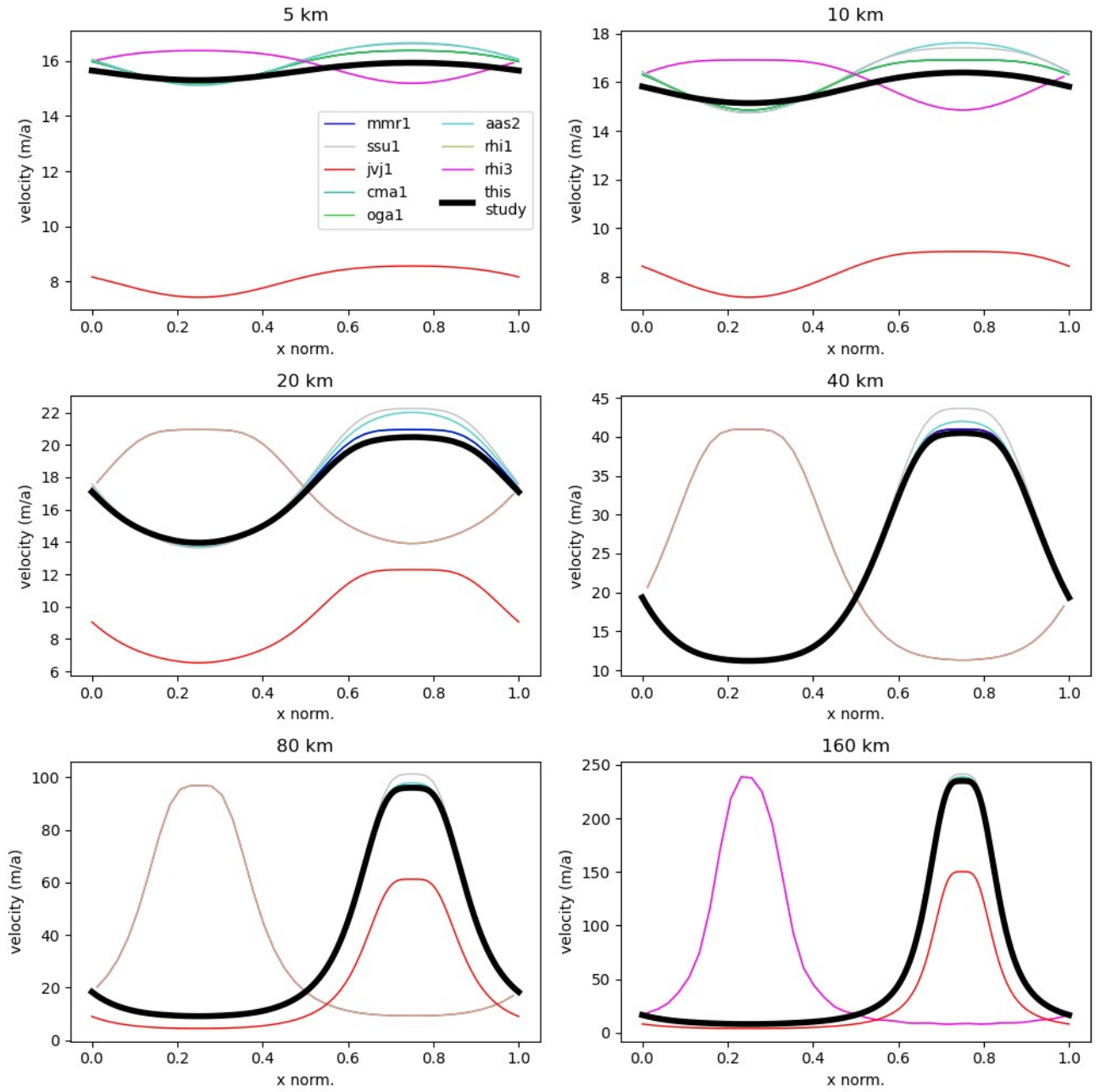
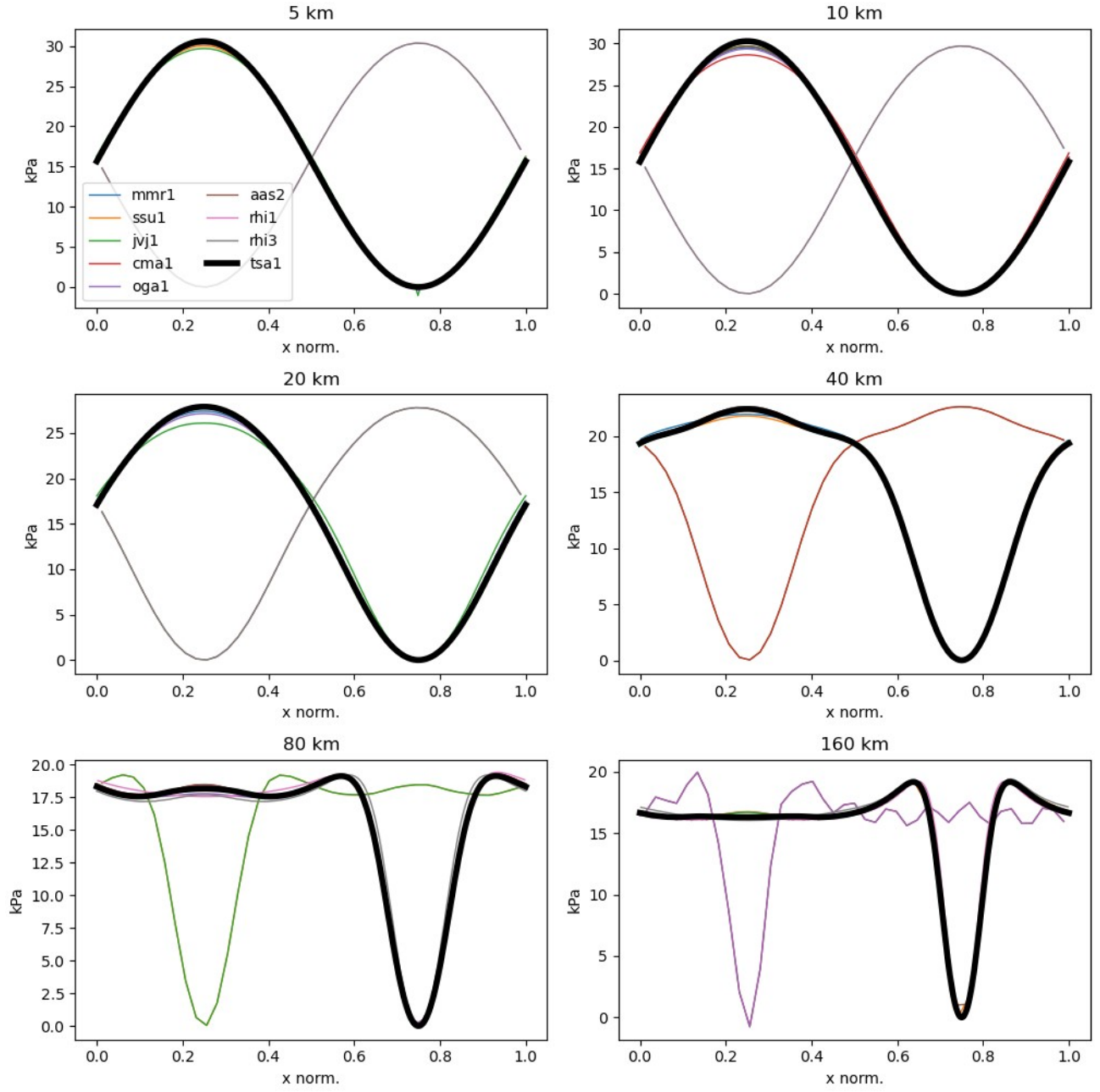


Figure S7: Experiment D. Velocity in x-direction at the surface,  $V_x(y_s)$ . Black line: this study (tsa1).



**Figure S8: Experiment D. Velocity in  $x$ -direction at the basis,  $v_x(y_b)$ . Black line: this study (tsa1).**



**Figure S9: Experiment D. Shear stress in x-direction at the basis,  $\tau_{xy}(y_b)$ . Black line: this study (tsa1).**

## 6 Diagrams for Experiment E

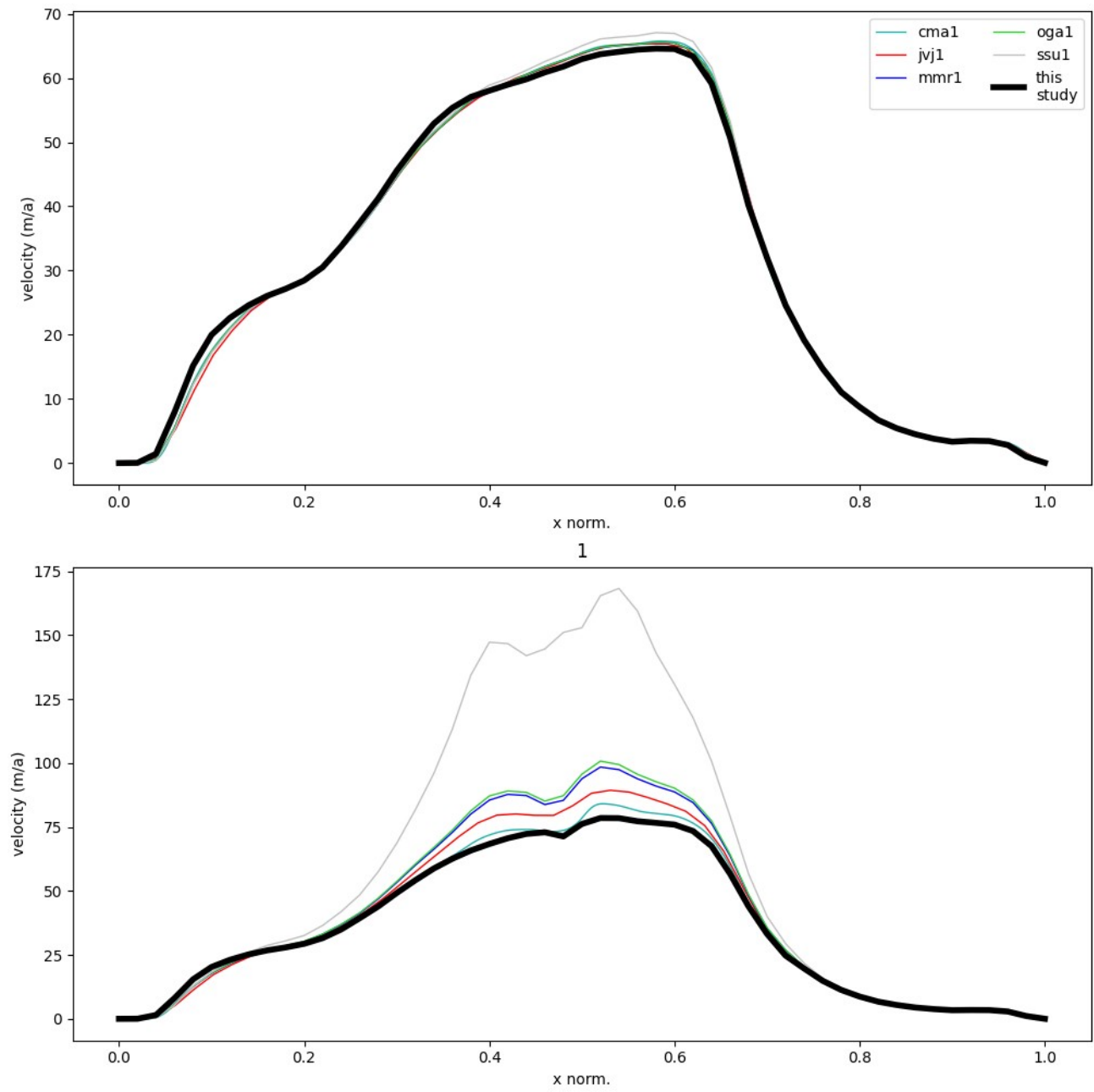


**Figure S10: Experiment E. Surface velocity in x-direction,  $v_x(y_s)$ . Black line: this study (jla1). Top: no-sliding experiment. Bottom: a narrow zone of zero traction exists close to the center.**

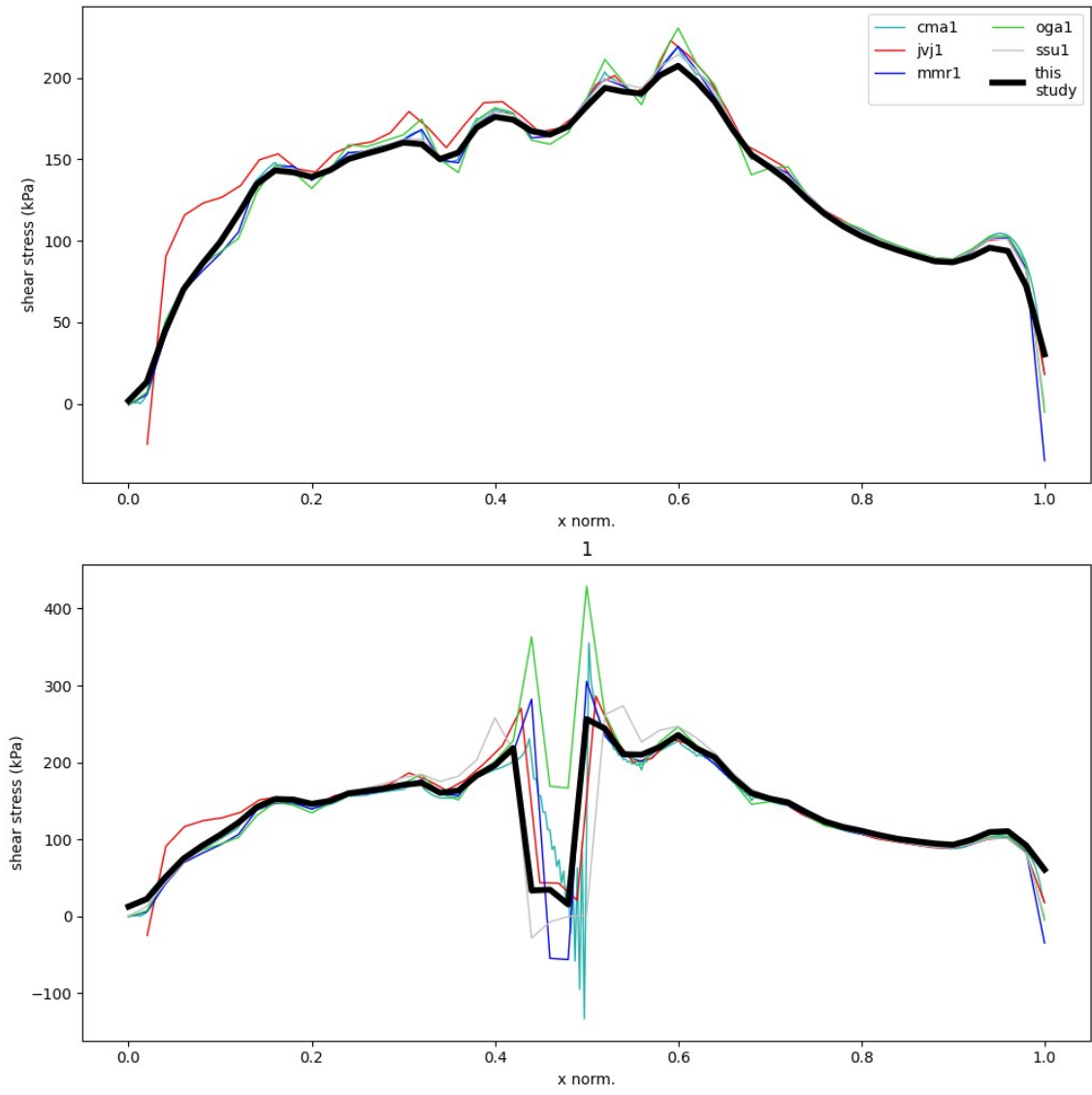


**Figure S11: Experiment E. Basal shear stress  $\tau_{xy}(y_b)$  in direction of ice flow. Top: no-sliding experiment. Bottom: a narrow zone of zero traction exists close to the center.**

## 7 Diagrams for Experiment F

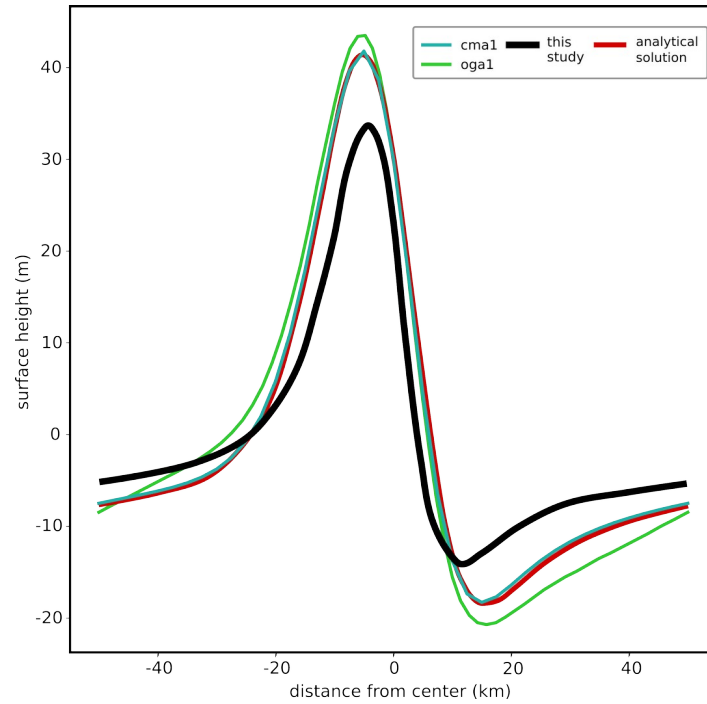


**Figure S12:** Experiment F. Surface height as a function of distance from the central Gaussian bump, flow occurs parallel to  $x$ . Analytical solution contributed by Frank Pattyn (2022, personal communication).

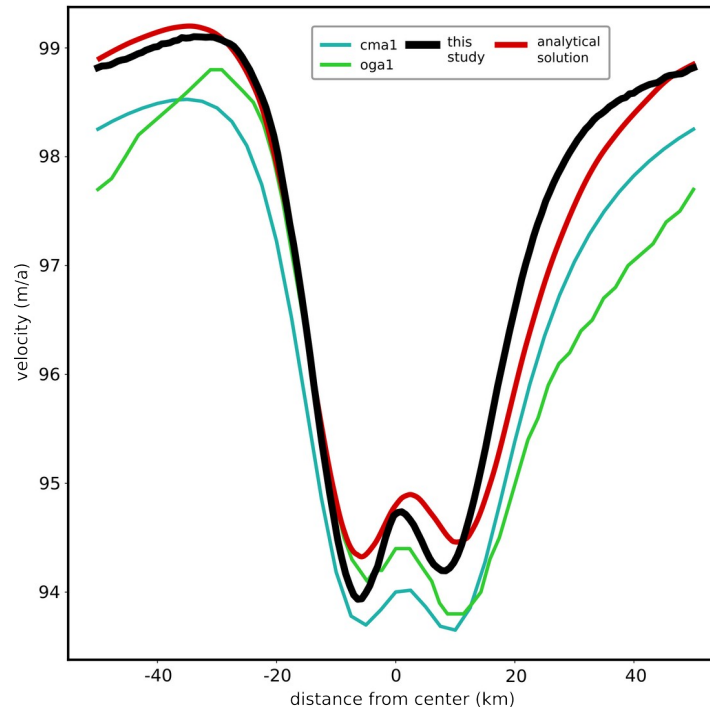


**Figure S13:** Experiment F. Surface velocity (in m/a) as a function of distance from the central Gaussian bump, flow occurs parallel to  $x$ . Analytical solution contributed by Frank Pattyn (2022, personal communication).



## References

- Gagliardini, O. and Zwinger, T.: The ISMIP-HOM benchmark experiments performed using the Finite-Element code Elmer, *The Cryosphere*, 2(1), 67–76, <https://doi.org/10.5194/tc-2-67-2008>, 2008.
- Hindmarsh, R. C. A.: A numerical comparison of approximations to the Stokes equations used in ice sheet and glacier modeling: HIGHER-ORDER GLACIER MODELS, *J. Geophys. Res.*, 109(F1), <https://doi.org/10.1029/2003JF000065>, 2004.
- Johnson, J. V. and Staiger, J. W.: Modeling long-term stability of the Ferrar Glacier, East Antarctica: Implications for interpreting cosmogenic nuclide inheritance, *J. Geophys. Res.*, 112(F3), F03S30, <https://doi.org/10.1029/2006JF000599>, 2007.
- Mansour, J., Giordani, J., Moresi, L., Beucher, R., Kaluza, O., Velic, M., Farrington, R., Quenette, S. and Beall, A.: Underworld2: Python Geodynamics Modelling for Desktop, HPC and Cloud, *JOSS*, 5(47), 1797, <https://doi.org/10.21105/joss.01797>, 2020.
- Martín, C., Navarro, F., Otero, J., Cuadrado, M. L. and Corcuera, M. I.: Three-dimensional modelling of the dynamics of Johnsons Glacier, Livingston Island, Antarctica, *Ann. Glaciol.*, 39, 1–8, <https://doi.org/10.3189/172756404781814537>, 2004.
- Pattyn, F., Perichon, L., Aschwanden, A., Breuer, B., de Smedt, B., Gagliardini, O., Gudmundsson, G. H., Hindmarsh, R. C. A., Hubbard, A., Johnson, J. V., Kleiner, T., Konovalov, Y., Martin, C., Payne, A. J., Pollard, D. and Price, S.: Benchmark experiments for higher-order and full-Stokes ice sheet, *The Cryosphere*, 16, 2008.
- Sugiyama, S., Gudmundsson, G. H. and Helbing, J.: Numerical investigation of the effects of temporal variations in basal lubrication on englacial strain-rate distribution, *Ann. Glaciol.*, 37, 49–54, <https://doi.org/10.3189/172756403781815618>, 2003.